



Geophysical Research Letters[®]

RESEARCH LETTER

10.1029/2025GL118737

Key Points:

- Spring Festival NOx reductions shifted from suppressing to enhancing ozone (2015–2024) despite similar emission reduction patterns
- Cloud cover and solar radiation explain 85%–94% of ozone response variability, while emission changes have minimal influence
- Meteorological control over ozone responses to emission reductions underscores the challenges of mitigation in a changing climate

Supporting Information:

Supporting Information may be found in the online version of this article.

Correspondence to:

Y. Wang,
yuhang.wang@eas.gatech.edu

Citation:

Zhao, F., Wang, Y., & Xi, S. (2025). Meteorological control on ozone response to NOx emission reduction events: Evidence from the Spring Festival periods. *Geophysical Research Letters*, 52, e2025GL118737. <https://doi.org/10.1029/2025GL118737>

Received 13 AUG 2025

Accepted 29 NOV 2025

Author Contributions:

Conceptualization: Fanghe Zhao, Yuhang Wang
Data curation: Fanghe Zhao
Formal analysis: Fanghe Zhao
Funding acquisition: Yuhang Wang
Investigation: Fanghe Zhao
Methodology: Fanghe Zhao
Project administration: Yuhang Wang
Resources: Fanghe Zhao, Yuhang Wang
Software: Fanghe Zhao
Supervision: Yuhang Wang
Validation: Fanghe Zhao
Visualization: Fanghe Zhao
Writing – original draft: Fanghe Zhao
Writing – review & editing:
 Fanghe Zhao, Yuhang Wang, Shengjun Xi

© 2025. The Author(s).

This is an open access article under the terms of the [Creative Commons](#)

[Attribution](#) License, which permits use, distribution and reproduction in any medium, provided the original work is properly cited.

Meteorological Control on Ozone Response to NOx Emission Reduction Events: Evidence From the Spring Festival Periods

Fanghe Zhao¹ , Yuhang Wang¹ , and Shengjun Xi¹

¹Georgia Institute of Technology, School of Earth and Atmospheric Sciences, Atlanta, GA, USA

Abstract China's Spring Festival, with consistent ~30% NO_x (NO + NO₂) reductions annually, provides a natural experiment to investigate oxidant response to emission reductions. Unlike isolated events such as the COVID-19 lockdown, the Spring Festivals offer a more robust decade-long (2015–2024) data set. Analysis of these observations reveals a striking shift in oxidant (Ox = O₃ + NO₂) response from negative to positive values over time despite similar emission reduction patterns each year. Chemical transport modeling indicates that meteorological factors are the primary drivers of these variations. Machine learning analysis further identifies cloud cover and radiation changes as controlling factors, with strong correlations between ΔOx and meteorological parameters ($R = 0.85–0.94$) across all regions. These findings challenge conventional assumptions about emission control effectiveness, showing that meteorological variability overrides expected chemical responses. Our results indicate that emission reduction policies must adaptively account for meteorological conditions to effectively mitigate ozone pollution in a changing climate.

Plain Language Summary During China's annual Spring Festival period, nationwide factory shutdowns and traffic reductions create a natural experiment with ~30% drops in nitrogen oxide (NO_x) emissions. Our decade-long analysis (2015–2024) reveals a surprising reversal pattern: ozone responses to the same NO_x reductions have shifted from decreasing to increasing over time. Using numerical models and machine learning, we discovered that weather conditions—particularly cloud cover and incoming solar radiation—control ozone changes far more than emission changes themselves. When Spring Festival periods coincide with clearer skies than surrounding weeks, increased solar radiation enhances ozone despite lower NO_x; cloudier conditions suppress ozone under similar emission reduction conditions. Our results underscore the need for adaptive ozone mitigation strategies that account for meteorological variability, not just emission reduction targets—a critical insight as cities worldwide face growing challenges in controlling ozone pollution amid a changing climate.

1. Introduction

Tropospheric ozone pollution represents a significant global challenge for both human health and ecosystem function (Lu et al., 2018, 2020; Manisalidis et al., 2020). Understanding the complex formation mechanisms of this secondary pollutant is crucial for developing effective control strategies. In recent decades, atmospheric scientists have established that ozone forms through complex nonlinear photochemical reactions involving nitrogen oxides (NO_x) and volatile organic compounds (VOCs) as primary precursors, modulated by photolysis rates, water vapor, HONO chemistry, and aerosol interactions, yet the precise relationships governing these interactions continue to challenge pollution control efforts worldwide (Liu & Shi, 2021; Ren et al., 2022; Tan et al., 2018; Wang et al., 2019).

Natural experiments of large-scale emission reductions provide unique opportunities to investigate these chemical relationships under real-world conditions. The Chinese Spring Festival (Lunar New Year) represents one such experiment, characterized by nationwide industrial shutdowns and transportation reductions that typically result in 30%–50% decreases in NO_x emissions (Huang et al., 2012; Wu et al., 2022). These substantial but temporary changes in emission patterns create an ideal laboratory for studying atmospheric oxidant responses to emission reductions, particularly regarding ozone formation chemistry. The complex relationship between NO_x reductions and ozone formation poses challenges in megacities worldwide (Kleinman et al., 2002; Sicard et al., 2020), with additional complexity in China from high aerosol loadings (K. Li et al., 2019; Sharma et al., 2020). As countries

worldwide implement increasingly stringent emission control policies, understanding the meteorological factors that modulate their effectiveness becomes critical for global air quality management (Cooper et al., 2020).

Previous studies examining ozone sensitivity during Spring Festival periods have reported varying findings across different regions of China. Several researchers observed increased ozone concentrations despite NO_x reductions in most regions, leading to conclusions about VOC-limited chemical regimes (Dai et al., 2021; Shi et al., 2021). However, growing evidence suggests significant meteorological influences on these observations. Wang et al. (2020) identified substantial meteorology-induced biases in NO₂ profiles when examining human activity changes based on satellite data from a single year, demonstrating that meteorological variability can confound even the quantification of emission changes. Using Generalized Additive Models, Gong et al. (2018) demonstrated that meteorological factors could explain 43%–90% of ozone variation. More recently, Shen et al. (2024) found that during the COVID-19 lockdown, specific meteorological conditions—elevated temperatures, low relative humidity, and stagnant winds under persistent high-pressure systems—critically modulated ozone levels, often counteracting the benefits of reduced precursor emissions. Increased light availability enhances photolysis rates, thereby increasing radical production and ozone formation from the same amount of NO_x and VOC precursors. This critical knowledge gap, the lack of systematic analysis of ozone response to emission reductions (Wang et al., 2022), has prevented a comprehensive understanding of whether observed changes primarily reflect emission-induced chemical regime characteristics or meteorological variations.

To address this knowledge gap, we examined the oxidant (Ox) response to NO_x reductions during Spring Festival periods across a decade-long timeframe (2015–2024). We focus on Ox rather than O₃ alone because Ox is conserved with respect to the rapid recycling in the NO_x family, allowing us to isolate actual photochemical oxidant production changes from local titration effects (Lee et al., 2020; Souri et al., 2021; Wyche et al., 2021). This is particularly important during emission reduction events when decreased NO emissions can increase O₃ through reduced titration without representing genuine changes in photochemical oxidant production. Specifically, we aim to: (a) quantify long-term variations in the Ox response to consistent NO_x reductions during Spring Festival periods; (b) determine the relative contributions of emission changes versus meteorological variations to these observed variations, recognizing that meteorological conditions themselves modulate photochemical regimes; and (c) identify the specific meteorological parameters most responsible for modulating oxidant responses. Our findings highlight the dominant influence of meteorological factors, especially radiation variability due to cloud cover, over potential emission-induced chemical regime change in shaping ozone responses to emission reductions. Specifically, we demonstrate that meteorological variability can overwhelm emission-induced chemical signals during emission reduction events, complicating the interpretation of such events solely in terms of chemical regime characterization. These results provide crucial insights for developing more effective, meteorologically informed air quality management strategies worldwide.

2. Materials and Methods

2.1. Data Sources and Processing

We obtained air quality observations from the China National Environmental Monitoring Center (CNEMC) network (China National Environmental Monitoring Center Network, 2018; Kong et al., 2021), which comprises 1,702 monitoring stations distributed across China for the period 2015–2024. We accessed hourly measurements of NO₂ and O₃ concentrations, which underwent strict quality control procedures to ensure data integrity. Our analysis required that at least 75% hourly measurements are available for each defined period (pre-, during-, and post-Spring Festival) to meet data completeness criteria, following completeness thresholds used in previous air quality and environmental monitoring studies (Fontes et al., 2017; Li et al., 2013; Liu et al., 2022; Ma et al., 2011). To account for the rapid photochemical cycling between NO₂ and O₃, we calculated the Ox (O₃ + NO₂) concentration at each site (Wang et al., 2023). We categorized monitoring sites into four geographical regions: Northwest (NW, 296 sites), Northeast (NE, 714 sites), Southwest (SW, 149 sites), and Southeast (SE, 480 sites), with site distributions presented in Figure S1 of Supporting Information S1.

To evaluate differences between Spring Festival and non-Festival periods, we used the following formula:

$$\Delta X = X_{\text{sf}} - \frac{1}{2}(X_{\text{pre}} + X_{\text{post}})$$

where X_{sf} , X_{pre} , and X_{post} denote values for 14-day periods during, before, and after the Spring Festival, respectively. We define an oxidant response sensitivity as the ratio of Ox change to that of NO_2 , $\frac{\Delta\text{Ox}}{\Delta\text{NO}_2}$. Regional ratio values were computed using the median values of individual sites to minimize the influence of extreme values. O_3 concentrations are represented by the maximum daily 8-hr average (MDA8) O_3 . NO_2 concentrations are calculated as the daily daytime 8-hr average. Ox presented in this study is calculated as the sum of MDA8 O_3 and the daily daytime 8-hr average NO_2 .

We chose $\Delta\text{Ox}/\Delta\text{NO}_2$ as our primary metric for several reasons. First, it can be calculated directly from routine observational data (O_3 and NO_2) available from the nationwide monitoring network, enabling systematic analysis across 1,702 sites over a decade without requiring model simulations or measurements of chemical species not routinely monitored. Second, it provides a measure of overall odd-oxygen sensitivity to emission-induced NO_2 perturbations since using Ox reduces variability associated with the fast $\text{NO}-\text{NO}_2-\text{O}_3$ cycling driven by photolysis of NO_2 to NO and the formation of NO_2 from the reaction of NO and O_3 . Third, our primary objective is to demonstrate that meteorological variability, rather than emission changes or the resulting shifts in chemical regimes, dominates observed oxidant responses during emission reduction events. For this purpose, using the observation-based $\Delta\text{Ox}/\Delta\text{NO}_2$ metric is advantageous, as it allows us to examine year-to-year variations without introducing model uncertainties or non-routinely measured compounds in this observational-based analysis.

It is important to emphasize that we use $\Delta\text{Ox}/\Delta\text{NO}_2$ primarily as an observational indicator to track temporal variations in oxidant responses across years, rather than as a definitive diagnostic of chemical regimes. At the same time, the observed $\Delta\text{Ox}/\Delta\text{NO}_2$ ratio remains valuable during periods of substantial emission reductions, such as the Spring Festival or the COVID-19 lockdown, when NO_2 concentrations decline markedly. In such cases, any increase in Ox necessarily yields a negative $\Delta\text{Ox}/\Delta\text{NO}_2$. Quantifying the frequency and magnitude of Ox increases relative to precursor reductions, whether driven by chemical-regime shifts or meteorological changes, is therefore a critical component of our analysis. Furthermore, the mechanistic interpretation of these variations is supported by our machine-learning analysis (Section 2.2) and chemical-transport model simulations (Section 2.3), which explicitly represent photochemical, meteorological, emission, and deposition processes.

To quantify long-term trends in ΔOx and meteorological parameters, we employed the Theil-Sen estimator (Theil, 1992), a robust non-parametric trend analysis method particularly suitable for environmental time series data. This approach calculates the median of slopes between all pairs of points in the time series, providing resistance to outliers and non-normal data distributions while maintaining reliability with up to $\sim 30\%$ outliers in the data set (Rousseeuw, 1987).

We obtained meteorological variables from the ECMWF Reanalysis v5 (ERA5) data set ($0.25^\circ \times 0.25^\circ$ spatial resolution; Hersbach et al., 2020). Key parameters included temperature, relative humidity, cloud cover fraction, shortwave radiation, precipitation, wind speed, and boundary layer height. All meteorological variables were spatially interpolated to air quality monitoring station locations using bilinear interpolation to ensure correspondence between air quality and meteorological data (Kirkland, 2010).

2.2. Machine Learning Framework

We employed an XGBoost machine learning model (Chen & Guestrin, 2016) to analyze relationships between meteorological factors and ΔOx across regions. We configured the model with 500 estimators and a maximum depth of 6 to capture complex relationships while preventing overfitting based on the Bayesian search (Klein et al., 2017). The model was trained on 70% of the data, with 15% allocated for validation and 15% for testing. Model inputs included temperature, relative humidity, cloud cover fraction, shortwave radiation, precipitation, wind speed, and boundary layer height for pre-, during-, and post-Festival periods. We optimized hyperparameters through exhaustive grid search to maximize predictive performance (Ahmad et al., 2022).

The evaluation of the machine learning model (Figure S2a in Supporting Information S1) demonstrates good correlation on the evaluation data set ($R^2 = 0.78$). The cross-validation on 10-fold separation (Lumumba et al., 2024) of the training set (Figure S2b in Supporting Information S1) shows the stability of the model across different training partitions. We employed permutation importance according to Spearman ranking correlation (Nirmalraj et al., 2023) to validate that all selected features contribute meaningfully to model performance (Figure S3 in Supporting Information S1). This analysis revealed that downward UV radiation at the surface was the most

important predictor of ΔOx response. Model training and validation procedures are detailed in Text S1 of Supporting Information S1.

To interpret the machine learning results, we employed Shapley Additive exPlanations (SHAP) analysis, a game theory-based approach that quantifies each input feature's contribution to model predictions while maintaining local accuracy and consistency properties (Chen et al., 2022; Lundberg & Lee, 2017; Scott & Lundberg, 2017). For our tree-based XGBoost model, we utilized TreeExplainer to efficiently compute SHAP values for each meteorological feature across all instances in our data set (Lundberg et al., 2020). This approach enabled quantification of the marginal contribution of individual variables to ΔOx predictions while preserving the complex, non-linear relationships captured by the model.

2.3. Regional Atmospheric Chemistry Transport Model

We employed the Regional chEmical and trAnsport Model (REAM) to simulate atmospheric chemical processes and validate the meteorological influences identified through statistical analysis. This model has been extensively validated in numerous atmospheric chemistry studies (Chong et al., 2024; Li et al., 2021; J. Li et al., 2019; Liu et al., 2012; Qu et al., 2021; Yan et al., 2021). The model domain covered China with a horizontal resolution of 36 km \times 36 km and 30 vertical layers. Meteorological fields were driven by WRF-ARW v4 (Weather Research and Forecasting) model simulations constrained by ERA5 data (Hersbach et al., 2020). Background anthropogenic emissions were based on the Multi-resolution Emission Inventory for China (MEIC) (Zheng et al., 2021).

To investigate whether the observed variations were driven by meteorology, we conducted simulations using 2017 MEIC emissions and the same Spring Festival emission adjustments with varying meteorological conditions for 2015–2024. During the Spring Festival period, NOx emissions were reduced by 30%, followed by a 10% reduction in the post-Festival period, while VOC emissions decreased by 10% during the festival, following established protocols from previous studies (Dai et al., 2021). This experimental design effectively isolated the impacts of meteorological variations on ozone formation and its sensitivity to NOx reductions, allowing us to quantify the meteorological contribution to observed ozone changes during the 10 spring festival periods. For comparison purposes, we also carried out sensitivity simulations for the Spring Festival periods using MEIC emissions from 2015 to 2020 but with the same meteorology for 2017.

3. Results

3.1. Long-Term Variations of Oxidant Response Sensitivities

All $\Delta\text{Ox}/\Delta\text{NO}_2$ values reported in this subsection are calculated from observed surface measurements from the CNEMC monitoring network unless otherwise specified. For the purpose of illustration, we apply the Theil-Sen estimator (Theil, 1992) to compute the trends of observed Ox to NOx emission reductions during the Spring Festival periods. Analysis of oxidant response sensitivities ($\Delta\text{Ox}/\Delta\text{NO}_2$) to changes in NO_2 concentrations revealed interannual variability with overall declining patterns across China during 2015–2024. The observed national $\Delta\text{Ox}/\Delta\text{NO}_2$ ratio exhibited a marked decreasing trend ($-0.16/\text{yr}$), with a total reduction of 63% over the decade (Figure S4 in Supporting Information S1). This ratio decreased from positive values to near zero, indicating diminished oxidant sensitivity to NO_x emission reductions, with particularly low values observed during and after the COVID-19 pandemic period (2020 onward) when emission reductions were further intensified.

Regional analysis revealed distinct spatial patterns in oxidant response sensitivity across China. Three of the four major regions (Northwest, Northeast, and Southeast) exhibited decreasing patterns in $\Delta\text{Ox}/\Delta\text{NO}_2$, while the Southwest showed more variable patterns without a clear linear trend, though values in all regions generally transitioned from predominantly positive in earlier years to near-zero or negative by 2024 (Figure 1 and Figure S5 in Supporting Information S1). Regional patterns show that the Southeast and Southwest regions exhibited more variable $\Delta\text{Ox}/\Delta\text{NO}_2$ values compared to Northwest and Northeast regions (Figure S5 in Supporting Information S1), though the statistical significance of individual regional trends is limited ($p > 0.05$) due to substantial interannual variability. Notably, the proportion of monitoring sites exhibiting positive $\Delta\text{Ox}/\Delta\text{NO}_2$ values decreased from 2015 to 2024 in the same order: 70% in Southwest, 40% in Southeast, 35% in Northwest, and 10% in Northeast (Figure 1). Figure 1 shows the regional responses distribution of the fractions of sites with positive versus negative $\Delta\text{Ox}/\Delta\text{NO}_2$, while Figure S5 in Supporting Information S1 presents the regional median magnitudes, which can be skewed by ΔNO_2 values close to 0. For example, the median $\Delta\text{Ox}/\Delta\text{NO}_2$ values for 2020

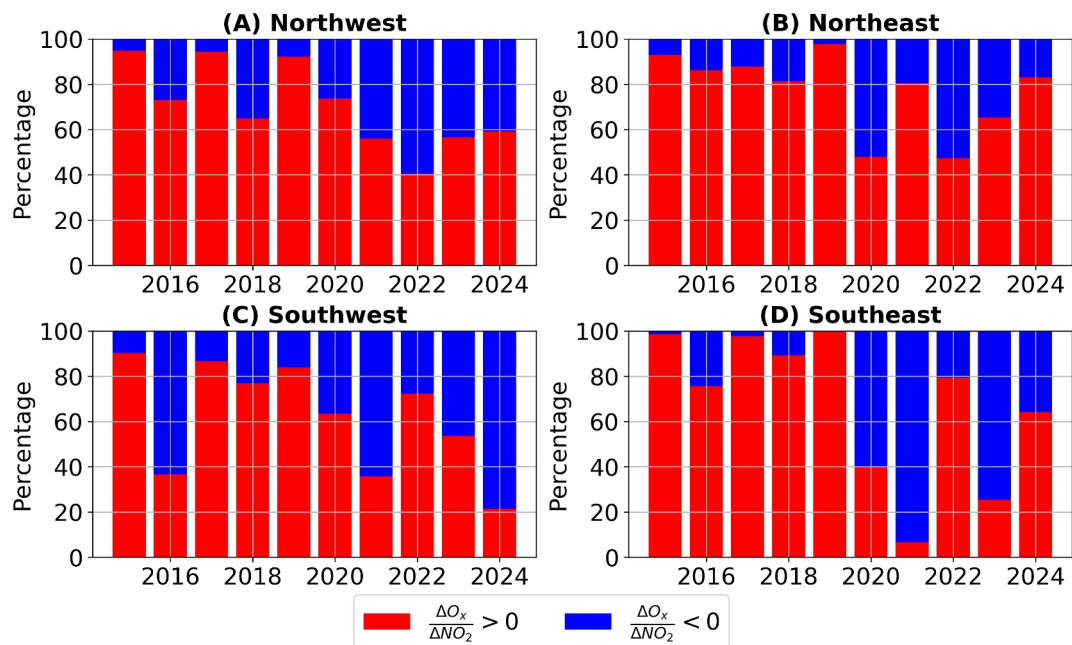


Figure 1. Regional variations in oxidant response sensitivity to NO_x reductions across China (2015–2024). Annual percentage of monitoring sites with positive (red) and negative (blue) $\Delta\text{Ox}/\Delta\text{NO}_2$ ratios in four major regions: (a) Northwest China (NW), (b) Northeast China (NE), (c) Southwest China (SW), and (d) Southeast China (SE). The figure demonstrates the shifting patterns in oxidant sensitivity to NO_x reductions across different regions of China over the decade-long study period.

and 2022 in the Northeast region are close to 0 and slightly negative and the 2022 values are more negative (Figure S5 in Supporting Information S1). In comparison, the corresponding negative $\Delta\text{Ox}/\Delta\text{NO}_2$ fractions are slightly $>50\%$ but are essentially the same (Figure 1).

Provincial-level analysis indicated that approximately 92% of monitoring sites experienced decreasing $\Delta\text{Ox}/\Delta\text{NO}_2$ values over the study period (Figure S6 in Supporting Information S1), with the strongest decreases observed in southern regions. Importantly, NO_2 reductions during Spring Festival remained stable at 12%–20% across all regions throughout the decade, consistent with previous research (Dai et al., 2021; Javed et al., 2021; Li et al., 2021). This stability suggests that the changing $\Delta\text{Ox}/\Delta\text{NO}_2$ ratios primarily reflect changes in ΔOx rather than variations in emission reduction patterns.

Further analysis of absolute ΔOx values further confirmed this interpretation, revealing significant increases from large negative values to near-zero or small positive values across the study period. The national ΔOx exhibited an increasing trend of 0.92 ppbV/yr (Figure S4 in Supporting Information S1). The Northwest region showed an increasing ΔOx pattern of 0.97 ppbV/yr; the Northeast region increased at 0.52 ppbV/yr; the Southwest region increased at 1.21 ppbV/yr; and the Southeast region increased at 1.18 ppbV/yr (Figure 2).

The analysis above provides a straightforward overview of oxidant response patterns during the Spring Festival periods. However, it is important to note that the statistical significance of most linear trends, as indicated by their p -values, is limited, with many values exceeding 0.05. Notably, the national $\Delta\text{Ox}/\Delta\text{NO}_2$ ratio shows a significant decreasing trend ($p = 0.02$), and the Northwest region exhibits a significant increasing trend in ΔOx ($p < 0.01$). The remaining patterns have p -values ranging from 0.06 to 0.2, reflecting substantial interannual variability in oxidant responses. To reduce the p -values, a considerably longer observation period is necessary.

To further assess the statistical significance of these changes, we grouped data from the first and last 5 years in each region and performed t -tests to evaluate the differences between the two periods. The analysis revealed significantly higher ΔOx levels in the last 5 years compared to the first 5 years across all four regions and total China ($p < 0.001$; Figure S7 in Supporting Information S1). Given that the large variability in the $\Delta\text{Ox}/\Delta\text{NO}_2$ ratio could introduce analytical uncertainties, we examined the fraction of sites exhibiting positive $\Delta\text{Ox}/\Delta\text{NO}_2$ ratios as a more robust indicator for ratio changes. The analysis showed significant decreases in the positive $\Delta\text{Ox}/\Delta\text{NO}_2$

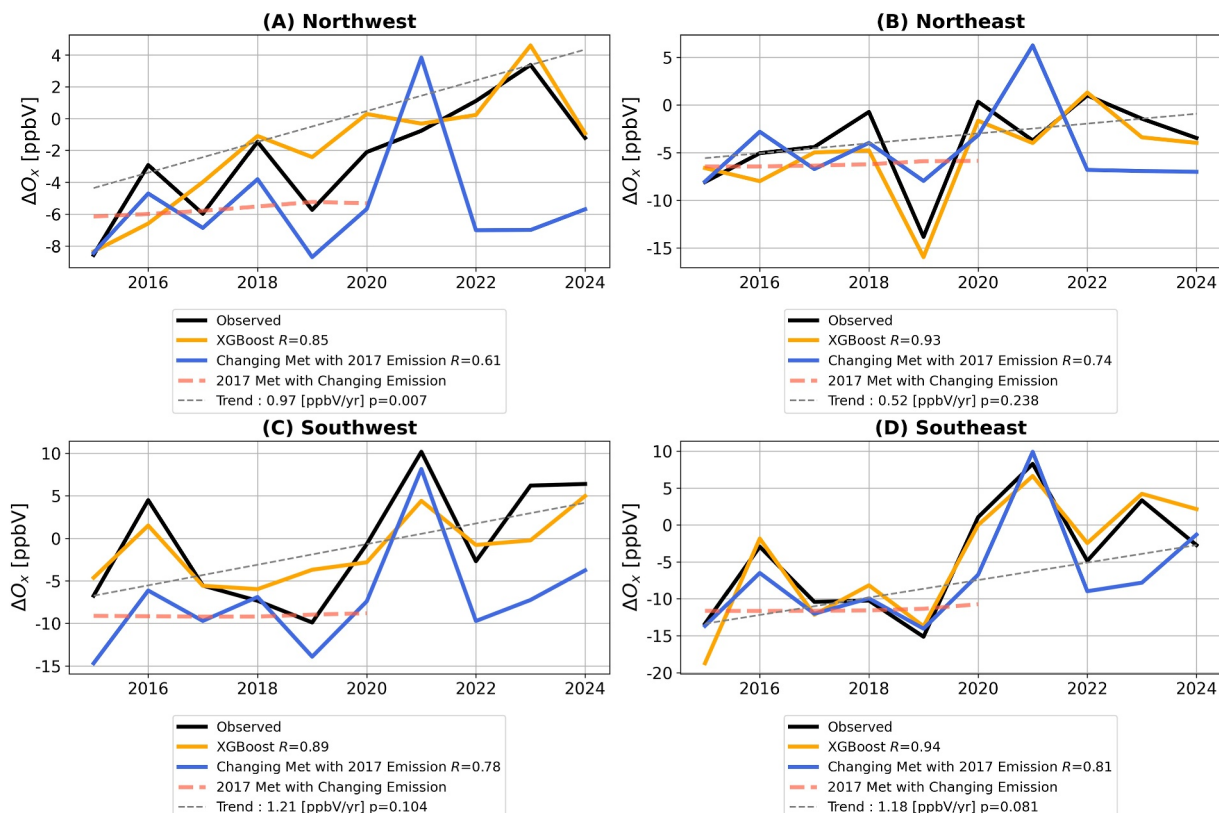


Figure 2. Observed and modeled ΔOx variations during Spring Festival periods across China (2015–2024). Time series showing observed ΔOx values (black line), model simulations with fixed emission reductions but varying meteorology (blue line), machine learning model predictions based on meteorological factors (yellow line), model simulations with fixed 2017 meteorology but yearly varying emissions from 2015 to 2020 (pink dash line, limited to 2020 due to public emission inventory availability) for: (a) Northwest, (b) Northeast, (c) Southwest, and (d) Southeast. Correlation coefficients between observations and predicted values are shown in the legend.

site fraction between the two periods for all regions ($p < 0.02$) except Southwest China, where the p -value is 0.095; Figure S8 in Supporting Information S1). In the next section, we focus on the meteorological contributions to the observed variations in oxidant responses.

3.2. Meteorological Control of Oxidant Response

To elucidate the mechanisms driving ΔOx changes, we compared observed variations with chemical transport model simulations that used fixed emission reduction patterns but varied meteorological conditions. The model reproduced the observed variations across all regions, with correlation coefficients of 0.74 in the Northeast, 0.78 in the Southwest, 0.61 in the Northwest, and 0.81 in the Southeast (Figure 2). This finding provides strong evidence that meteorological variations, rather than changes in emission patterns or chemical regimes, primarily drive the observed trends in oxidant response. Because the model explicitly simulates chemistry, transport, emission, and deposition processes, the agreement between modeled and observed ΔOx variations demonstrates that meteorological influences on these processes, not changes in emission characteristics, are the primary drivers for the observed Ox variation patterns.

To further evaluate the effect of yearly emission changes on the observed oxidant response during Spring Festival periods, we conducted model simulations using yearly MEIC emissions from 2015 to 2020 with the same Spring Festival emission reduction pattern as in previous simulations. The same meteorological data for 2017 were used in all simulations since the observed ozone responses in 2017 were about average for the period of 2015–2020 (Figure 2). Despite substantial changes in emissions from 2015 to 2020, the resulting ΔOx variations remained minimal (Figure 2), demonstrating that yearly emission reductions cannot account for the magnitude or temporal variations of observed oxidant changes during the Spring Festival periods. These findings indicate that

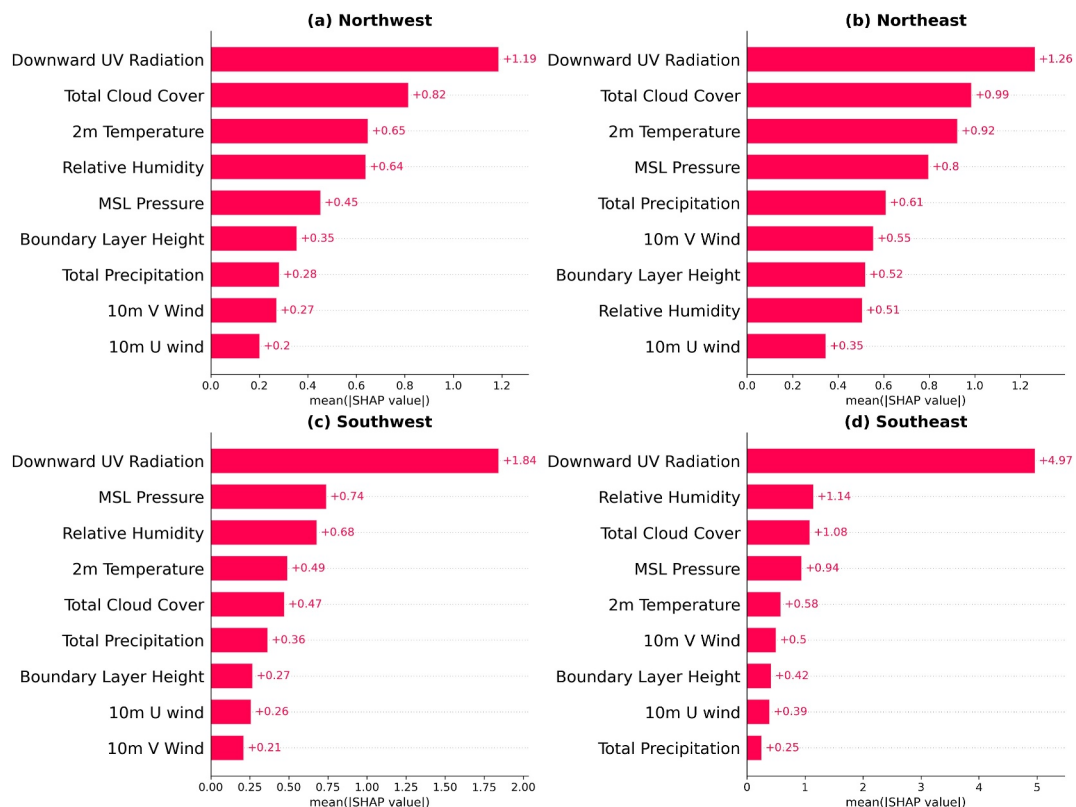


Figure 3. SHAP analysis of meteorological factors influencing ΔOx across four regions of China. Bar plots showing the mean absolute SHAP values for each meteorological predictor in the XGBoost model for: (a) Northwest, (b) Northeast, (c) Southwest, and (d) Southeast. Higher SHAP values indicate greater influence on model predictions. Across all regions, downward UV radiation consistently emerges as the dominant factor, followed by total cloud cover.

meteorological factors, rather than yearly emission changes, primarily drive the oxidant responses during Spring Festival episodes. Additional details of the emission sensitivity simulations are provided in Text S2 of Supporting Information S1.

Our chemical transport model simulations explicitly represent regional transport processes. The ability to reproduce the observed ΔOx variations using fixed emission patterns but varying meteorology demonstrates that meteorological influences on chemistry and transport are the primary drivers for the observed temporal variability. Emission-sensitivity simulations further show that substantial emission changes from 2015 to 2020, which would alter regional transport patterns through changed concentration gradients, produce minimal ΔOx variations under fixed meteorological conditions. These results indicate that meteorological modulation of photochemical processes and transport, not emission-driven changes, explains the observed oxidant response patterns.

Our machine learning approach further isolated meteorological influences on ΔOx , reproducing variations with correlation coefficients of 0.93 in the Northeast, 0.89 in the Southwest, 0.85 in the Northwest, and 0.94 in the Southeast (Figure 2). These results confirm that meteorological factors can explain the majority of observed variations in oxidant response to NO_x reductions.

SHAP analysis identified radiation differences as the most important predictors of ΔOx across all regions (Figure 3 and S3 in Supporting Information S1). In southern regions (Southeast and Southwest), downward UV radiation emerged as the dominant factor, with more than twice the impact of the second most important factor, while cloud cover ranked third in Southeast and fifth in Southwest. This finding suggests that ΔOx and atmospheric ozone chemistry during Spring Festival periods in southern China are primarily modulated by radiation changes. In northern China (Northwest and Northeast), both downward UV radiation and cloud cover ranked as the top two predictors, while temperature also influenced ΔOx , though with less explanatory power than radiation variables.

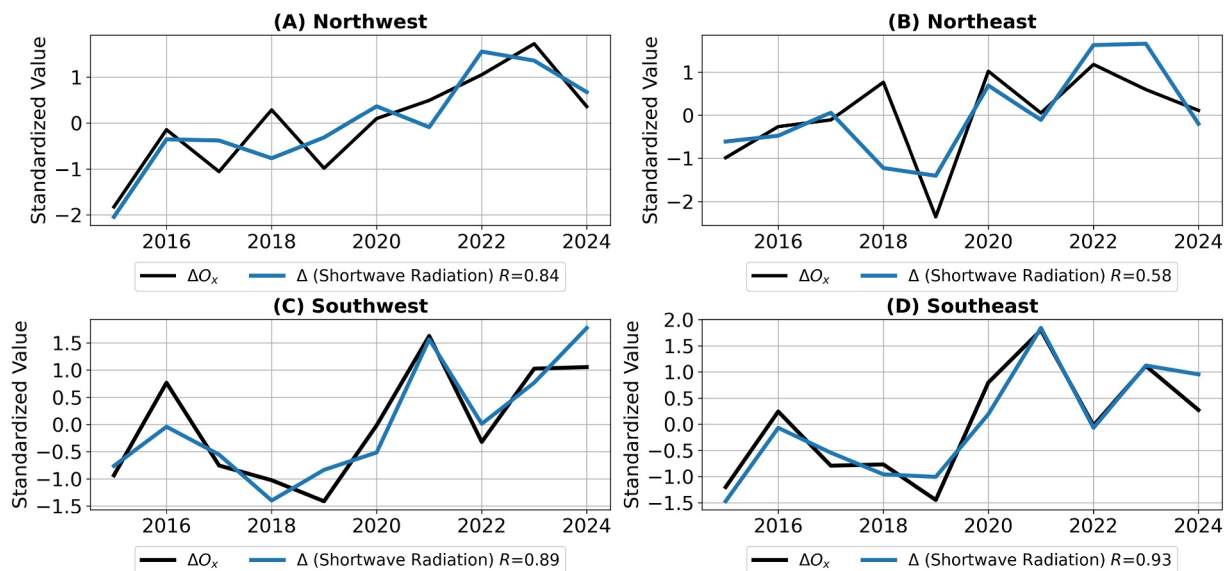


Figure 4. Temporal variations of z-score standardized ΔO_x and shortwave radiation differences across regions (2015–2024). Time series showing z-score standardized ΔO_x (black line) and z-score standardized Δ (Shortwave Radiation) (blue line) for the four regions. Correlation coefficients between the two variables are shown in the legend for each region.

3.3. Correlation Between Meteorological Factors and Oxidant Response

Quantitative analysis of the relationships between normalized ΔO_x and Δ Shortwave Radiation revealed strong correlations across all regions, with correlation coefficients of 0.84 for the Northwest, 0.58 for the Northeast, 0.89 for the Southwest, and 0.93 for the Southeast (Figure 4). The z-score standardization enables direct visual comparison of temporal patterns despite different variable units. These robust correlations confirm the critical role of radiation processes in controlling oxidant response during emission reduction periods.

The correlation analysis identified cloud cover as a primary meteorological driver behind radiation changes, with strong negative correlations between UV radiation differences and cloud cover across all regions (correlation coefficient of -0.90 for the Northwest, -0.84 for the Northeast, -0.90 for the Southwest, and -0.95 for the Southeast; Figure S9 in Supporting Information S1). In southern regions, UV radiation differences also strongly correlated with precipitation and relative humidity differences, which are themselves associated with cloud formation processes. These findings suggest that the observed interannual variations in ΔO_x are attributable in part to differences in cloud cover between Spring Festival and non-Festival periods, potentially influenced by reduced firework usage during Spring Festival (Liu et al., 2024; Yao et al., 2019) and regional climate (Xue et al., 2021; Zhang et al., 2024; Zhang & Wu, 2018).

The meteorological control documented above also explains regional differences in response magnitudes. Southern regions exhibited stronger patterns (Section 3.1) due to tighter coupling between ΔO_x and radiation variability ($R = 0.89\text{--}0.93$ vs. $0.58\text{--}0.84$ in the north, Figure 4) and greater UV radiation dominance (Figure 3). These patterns reflect southern China's larger interannual variability in spring downward UV radiation and cloud cover driven in part by higher moisture availability and warmer temperatures that amplify photochemical sensitivity to radiation changes.

4. Conclusions

Emission control policies worldwide increasingly target NO_x reduction to mitigate tropospheric ozone pollution, yet the efficacy of these interventions remains uncertain due to complex atmospheric chemistry. China's Spring Festival period each year, characterized by consistent NO_x reductions at $\sim 30\%$, serves as a natural experiment to investigate atmospheric oxidant response to emission reductions. The recurring and widespread nature of these emission reductions offers a larger and more robust data set than isolated long-duration events, such as the COVID-19 lockdown.

Our findings demonstrate that oxidant response to NO_x reductions during China's Spring Festival periods is predominantly controlled by meteorological variations rather than changes in chemical regimes, with cloud cover-driven radiation changes being an important controlling factor across all regions. These results highlight that meteorological variability can mask or overwhelm emission-induced chemical regime signals during emission reduction events, complicating the interpretation of such events for photochemical regime characterization (Sillman, 1999) and highlight the necessity of accounting for meteorological influences when assessing emission control policies (Cao et al., 2024; Mai et al., 2024; Sadeghi et al., 2022; Yang et al., 2025). As climate change can significantly alter regional meteorological patterns (Bolan et al., 2024; IPCC, 2023), the effectiveness of NO_x reduction strategies may decouple from emission characteristics. Future air quality management should incorporate meteorological considerations through adaptive control measures, while research efforts should focus on developing integrated climate-chemistry models to inform more resilient strategies in a changing climate.

Conflict of Interest

The authors declare no conflicts of interest relevant to this study.

Data Availability Statement

Air-quality observations used in this study are publicly available from the China National Environmental Monitoring Center (CNEMC; <https://www.cnemc.cn/en/>) with historical daily data accessible at Zhao (2025). The MEIC emission inventory can be accessed on the MEIC website (<http://www.meicmodel.org/>). Software for this research is available in these websites: <https://github.com/dmlc/xgboost>, <https://github.com/shap/shap>.

Acknowledgments

This work was supported in part by the National Science Foundation under Grant 2030425. We thank the China National Environmental Monitoring Centre for providing the nationwide air-pollutant measurement data that form the foundation of this study. We thank the MEIC team for making their 2015–2020 emission inventories publicly available. We would also like to acknowledge high-performance computing support from the Derecho system (<https://doi.org/10.5065/qq9a-pg09>) provided by the NSF National Center for Atmospheric Research (NCAR), sponsored by the National Science Foundation. This research was supported in part through research cyberinfrastructure resources and services provided by the Partnership for an Advanced Computing Environment (PACE) at the Georgia Institute of Technology, Atlanta, Georgia, USA.

References

Ahmad, G. N., Fatima, H., Ullah, S., Saidi, A. S., & Imdadullah (2022). Efficient medical diagnosis of human heart diseases using machine learning techniques with and without GridSearchCV. *IEEE Access*, 10, 80151–80173. <https://doi.org/10.1109/ACCESS.2022.3165792>

Bolan, S., Padhye, L. P., Jasemizad, T., Govarthanan, M., Karmegam, N., Wijesekara, H., et al. (2024). Impacts of climate change on the fate of contaminants through extreme weather events. *Science of the Total Environment*, 909, 168388. <https://doi.org/10.1016/j.scitotenv.2023.168388>

Cao, T., Wang, H., Chen, X., Li, L., Lu, X., Lu, K., & Fan, S. (2024). Rapid increase in spring ozone in the Pearl River Delta, China during 2013–2022. *npj Climate and Atmospheric Science*, 7(1), 309. <https://doi.org/10.1038/s41612-024-00847-3>

Chen, H., Lundberg, S. M., & Lee, S.-I. (2022). Explaining a series of models by propagating Shapley values. *Nature Communications*, 13(1), 4512. <https://doi.org/10.1038/s41467-022-31384-3>

Chen, T., & Guestrin, C. (2016). XGBoost: A Scalable tree boosting system. In *Proceedings of the 22nd ACM SIGKDD international conference on knowledge discovery and data mining* (pp. 785–794). <https://doi.org/10.1145/2939672.2939785>

China National Environmental. (2018). Monitoring center network. Retrieved from <http://www.cnemc.cn/>

Chong, K., Wang, Y., Zheng, M., Qu, H., Zhang, R., Lee, Y. R., et al. (2024). Observation-based diagnostics of reactive nitrogen recycling through HONO heterogenous production: Divergent implications for ozone production and emission control. *Environmental Science & Technology*, 58(26), 11554–11567. <https://doi.org/10.1021/acs.est.3c07967>

Cooper, O. R., Schultz, M. G., Schröder, S., Chang, K.-L., Gaudel, A., Benítez, G. C., et al. (2020). Multi-decadal surface ozone trends at globally distributed remote locations. *Elementa: Science of the Anthropocene*, 8, 23. <https://doi.org/10.1525/elementa.420>

Dai, Q., Hou, L., Liu, B., Zhang, Y., Song, C., Shi, Z., et al. (2021). Spring Festival and COVID-19 lockdown: Disentangling PM sources in major Chinese cities. *Geophysical Research Letters*, 48(11), e2021GL093403. <https://doi.org/10.1029/2021GL093403>

Fontes, T., Li, P., Barros, N., & Zhao, P. (2017). Trends of PM2.5 concentrations in China: A long term approach. *Journal of Environmental Management*, 196, 719–732. <https://doi.org/10.1016/j.jenvman.2017.03.074>

Gong, X., Hong, S., & Jaffe, D. A. (2018). Ozone in China: Spatial distribution and leading meteorological factors controlling O3 in 16 Chinese cities. *Aerosol and Air Quality Research*, 18(9), 2287–2300. <https://doi.org/10.4209/aaqr.2017.10.0368>

Hersbach, H., Bell, B., Berrisford, P., Hirahara, S., Horányi, A., Muñoz-Sabater, J., et al. (2020). The ERA5 global reanalysis. *Quarterly Journal of the Royal Meteorological Society*, 146(730), 1999–2049. <https://doi.org/10.1002/qj.3803>

Huang, K., Zhuang, G., Lin, Y., Wang, Q., Fu, J. S., Zhang, R., et al. (2012). Impact of anthropogenic emission on air quality over a megacity—revealed from an intensive atmospheric campaign during the Chinese Spring Festival. *Atmospheric Chemistry and Physics*, 12(23), 11631–11645. <https://doi.org/10.5194/acp-12-11631-2012>

IPCC. (2023). Climate change 2023: Synthesis report. Contribution of working groups I, II and III to the sixth assessment report of the intergovernmental panel on climate change.

Javed, Z., Tanvir, A., Wang, Y., Waqas, A., Xie, M., Abbas, A., et al. (2021). Quantifying the impacts of COVID-19 lockdown and Spring Festival on air quality over Yangtze River Delta Region. *Atmosphere*, 12(6), 735. <https://doi.org/10.3390/atmos12060735>

Kirkland, E. J. (2010). *Bilinear interpolation*. (pp. 261–263). Springer. https://doi.org/10.1007/978-1-4419-6533-2_12

Klein, A., Falkner, S., Bartels, S., Hennig, P., & Hutter, F. (2017). Fast Bayesian optimization of machine learning hyperparameters on large datasets. In *Proceedings of the 20th international conference on artificial intelligence and statistics, proceedings of machine learning research*. Retrieved from <https://proceedings.mlr.press/v54/klein17a.html>

Kleinman, L. I., Daum, P. H., Imre, D., Lee, Y. N., Nunnermacker, L. J., Springston, S. R., et al. (2002). Ozone production rate and hydrocarbon reactivity in 5 urban areas: A cause of high ozone concentration in Houston. *Geophysical Research Letters*, 29(10), 105-1. <https://doi.org/10.1029/2001GL014569>

Kong, L., Tang, X., Zhu, J., Wang, Z., Li, J., Wu, H., et al. (2021). A 6-year-long (2013–2018) high-resolution air quality reanalysis dataset in China based on the assimilation of surface observations from CNEMC. *Earth System Science Data*, 13(2), 529–570. <https://doi.org/10.5194/essd-13-529-2021>

Lee, J. D., Drysdale, W. S., Finch, D. P., Wilde, S. E., & Palmer, P. I. (2020). UK surface NO₂ levels dropped by 42% during the COVID-19 lockdown: Impact on surface O₃. *Atmospheric Chemistry and Physics*, 20(24), 15743–15759. <https://doi.org/10.5194/acp-20-15743-2020>

Li, D., Wu, Q., Wang, H., Xiao, H., Xu, Q., Wang, L., et al. (2021). The Spring Festival effect: The change in NO₂ column concentration in China caused by the migration of human activities. *Atmospheric Pollution Research*, 12(12), 101232. <https://doi.org/10.1016/j.apr.2021.101232>

Li, J., Wang, Y., & Qu, H. (2019). Dependence of summertime surface ozone on NO and VOC emissions over the United States: Peak time and value. *Geophysical Research Letters*, 46(6), 3540–3550. <https://doi.org/10.1029/2018GL081823>

Li, K., Jacob, D. J., Liao, H., Shen, L., Zhang, Q., & Bates, K. H. (2019). Anthropogenic drivers of 2013–2017 trends in summer surface ozone in China. *Proceedings of the National Academy of Sciences*, 116(2), 422–427. <https://doi.org/10.1073/pnas.1812168116>

Li, P., Xin, J., Wang, Y., Wang, S., Li, G., Pan, X., et al. (2013). The acute effects of fine particles on respiratory mortality and morbidity in Beijing, 2004–2009. *Environmental Science and Pollution Research*, 20(9), 6433–6444. <https://doi.org/10.1007/s11356-013-1688-8>

Liu, C., & Shi, K. (2021). A review on methodology in O₃-NO_x-VOC sensitivity study. *Environmental Pollution*, 291, 118249. <https://doi.org/10.1016/j.envpol.2021.118249>

Liu, X., Yang, L., Wang, Y., Yan, P., & Lu, Y. (2024). Effects of fireworks burning on air quality during the Chinese Spring Festival—Evidence from Zhengzhou, China. *Toxics*, 12(1), 23. <https://doi.org/10.3390/toxics12010023>

Liu, Z., Liu, C., Cui, Y., Liu, J., Zhang, H., Feng, Y., et al. (2022). Air pollution and refraining from visiting health facilities: A cross-sectional study of domestic migrants in China. *BMC Public Health*, 22(1), 2007. <https://doi.org/10.1186/s12889-022-14401-4>

Liu, Z., Wang, Y., Gu, D., Zhao, C., Huey, L. G., Stickel, R., et al. (2012). Summertime photochemistry during CAREBeijing-2007: RO_x budgets and O₃ formation. *Atmospheric Chemistry and Physics*, 12(16), 7737–7752. <https://doi.org/10.5194/acp-12-7737-2012>

Lu, X., Hong, J., Zhang, L., Cooper, O. R., Schultz, M. G., Xu, X., et al. (2018). Severe surface ozone pollution in China: A global perspective. *Environmental Science and Technology Letters*, 5(8), 487–494. <https://doi.org/10.1021/acs.estlett.8b00366>

Lu, X., Zhang, S., Xing, J., Wang, Y., Chen, W., Ding, D., et al. (2020). Progress of air pollution control in China and its challenges and opportunities in the ecological civilization era. *Engineering*, 6(12), 1423–1431. <https://doi.org/10.1016/j.eng.2020.03.014>

Lumumba, V., Kiprotich, D., Mpaine, M., Makenna, N., & Kavita, M. (2024). Comparative analysis of cross-validation techniques: LOOCV, K-folds cross-validation, and repeated K-folds cross-validation in machine learning models. *American Journal of Theoretical and Applied Statistics*, 13(5), 127–137. <https://doi.org/10.11648/j.ajtas.20241305.13>

Lundberg, S. M., Erion, G., Chen, H., DeGrave, A., Prutkin, J. M., Nair, B., et al. (2020). From local explanations to global understanding with explainable AI for trees. *Nature Machine Intelligence*, 2(1), 56–67. <https://doi.org/10.1038/s42256-019-0138-9>

Lundberg, S. M., & Lee, S.-I. (2017). A unified approach to interpreting model predictions. In *Proceedings of the 31st international conference on neural information processing systems*.

Ma, Y., Chen, R., Pan, G., Xu, X., Song, W., Chen, B., & Kan, H. (2011). Fine particulate air pollution and daily mortality in Shenyang, China. *Science of the Total Environment*, 409(13), 2473–2477. <https://doi.org/10.1016/j.scitotenv.2011.03.017>

Mai, Z., Shen, H., Zhang, A., Sun, H. Z., Zheng, L., Guo, J., et al. (2024). Convolutional neural networks facilitate process understanding of megacity ozone temporal variability. *Environmental Science & Technology*, 58(35), 15691–15701. <https://doi.org/10.1021/acs.est.3c07907>

Manisalidis, I., Stavropoulou, E., Stavropoulos, A., & Beitzoglou, E. (2020). Environmental and health impacts of air pollution: A review. *Frontiers in Public Health*, 8, 14. [Review]. <https://doi.org/10.3389/fpubh.2020.00014>

Nirmalraj, S., Antony, A. S. M., Srideviponmalar, P., Oliver, A. S., Velmurugan, K. J., Elanangai, V., & Nagarajan, G. (2023). Permutation feature importance-based fusion techniques for diabetes prediction. *Soft Computing*. <https://doi.org/10.1007/s00500-023-08041-y>

Qu, H., Wang, Y., Zhang, R., Liu, X., Huey, L. G., Sjostedt, S., et al. (2021). Chemical production of oxygenated volatile organic compounds strongly enhances boundary-layer oxidation chemistry and ozone production. *Environmental Science & Technology*, 55(20), 13718–13727. <https://doi.org/10.1021/acs.est.1c04489>

Ren, J., Guo, F., & Xie, S. (2022). Diagnosing ozone–NO_x–VOC sensitivity and revealing causes of ozone increases in China based on 2013–2021 satellite retrievals. *Atmospheric Chemistry and Physics*, 22(22), 15035–15047. <https://doi.org/10.5194/acp-22-15035-2022>

Rousseeuw, P. J. (1987). *Robust regression and outlier detection*. Wiley. <https://doi.org/10.1002/0471725382>

Sadeghi, B., Ghahremanloo, M., Mousavinezhad, S., Lops, Y., Pouyaei, A., & Choi, Y. (2022). Contributions of meteorology to ozone variations: Application of deep learning and the Kolmogorov-Zurbenko filter. *Environmental Pollution*, 310, 119863. <https://doi.org/10.1016/j.envpol.2022.119863>

Scott, M., & Lundberg, S.-I. L. (2017). A unified approach to interpreting ModelPredictions. <https://doi.org/10.48550/arxiv.1705.07874>

Sharma, S., Zhang, M., Anshika, Gao, J., Zhang, H., & Kota, S. H. (2020). Effect of restricted emissions during COVID-19 on air quality in India. *Science of the Total Environment*, 728, 138878. <https://doi.org/10.1016/j.scitotenv.2020.138878>

Shen, F., Hegglin, M. I., & Yuan, Y. (2024). Impact of weather patterns and meteorological factors on PM2.5 and O₃ responses to the COVID-19 lockdown in China. *Atmospheric Chemistry and Physics*, 24(11), 6539–6553. <https://doi.org/10.5194/acp-24-6539-2024>

Shi, Z., Song, C., Liu, B., Lu, G., Xu, J., Van Vu, T., et al. (2021). Abrupt but smaller than expected changes in surface air quality attributable to COVID-19 lockdowns. *Science Advances*, 7(3), eabd6696. <https://doi.org/10.1126/sciadv.eabd6696>

Sicard, P., De Marco, A., Agathokleous, E., Feng, Z., Xu, X., Paoletti, E., et al. (2020). Amplified ozone pollution in cities during the COVID-19 lockdown. *Science of the Total Environment*, 735, 139542. <https://doi.org/10.1016/j.scitotenv.2020.139542>

Sillman, S. (1999). The relation between ozone, NO_x and hydrocarbons in urban and polluted rural environments. *Atmospheric Environment*, 33(12), 1821–1845. [https://doi.org/10.1016/S1352-2310\(98\)00345-8](https://doi.org/10.1016/S1352-2310(98)00345-8)

Souri, A. H., Chance, K., Bak, J., Nowlan, C. R., González Abad, G., Jung, Y., et al. (2021). Unraveling pathways of elevated ozone induced by the 2020 lockdown in Europe by an observationally constrained regional model using TROPOMI. *Atmospheric Chemistry and Physics*, 21(24), 18227–18245. <https://doi.org/10.5194/acp-21-18227-2021>

Tan, Z., Lu, K., Dong, H., Hu, M., Li, X., Liu, Y., et al. (2018). Explicit diagnosis of the local ozone production rate and the ozone-NO_x-VOC sensitivities. *Science Bulletin*, 63(16), 1067–1076. <https://doi.org/10.1016/j.scib.2018.07.001>

Theil, H. (1992). A rank-invariant method of linear and polynomial regression analysis. In *Advanced studies in theoretical and applied econometrics* (Vol. 23, pp. 345–381). Springer. https://doi.org/10.1007/978-94-011-2546-8_20

Wang, N., Lyu, X., Deng, X., Huang, X., Jiang, F., & Ding, A. (2019). Aggravating O₃ pollution due to NO_x emission control in eastern China. *Science of the Total Environment*, 677, 732–744. <https://doi.org/10.1016/j.scitotenv.2019.04.388>

Wang, S., Su, H., Streets, D. G., Zhang, Q., Lu, Z., He, K., et al. (2020). Spring Festival points the way to cleaner air in China. *arXiv preprint arXiv:2004.08442*.

Wang, W., Parrish, D. D., Wang, S., Bao, F., Ni, R., Li, X., et al. (2022). Long-term trend of ozone pollution in China during 2014–2020: Distinct seasonal and spatial characteristics and ozone sensitivity. *Atmospheric Chemistry and Physics*, 22(13), 8935–8949. <https://doi.org/10.5194/acp-22-8935-2022>

Wang, Y., Xi, S., Zhao, F., Huey, L. G., & Zhu, T. (2023). Decreasing production and potential urban explosion of nighttime nitrate radicals amid emission reduction efforts. *Environmental Science & Technology*, 57(50), 21306–21312. <https://doi.org/10.1021/acs.est.3c09259>

Wu, G., Tian, W., Zhang, L., & Yang, H. (2022). The Chinese Spring Festival impact on air quality in China: A critical review. *International Journal of Environmental Research and Public Health*, 19(15), 9074. <https://doi.org/10.3390/ijerph19159074>

Wyche, K. P., Nichols, M., Parfitt, H., Beckett, P., Gregg, D. J., Smallbone, K. L., & Monks, P. S. (2021). Changes in ambient air quality and atmospheric composition and reactivity in the South East of the UK as a result of the COVID-19 lockdown. *Science of the Total Environment*, 755, 142526. <https://doi.org/10.1016/j.scitotenv.2020.142526>

Xue, W., Shi, X., Yan, G., Wang, J., Xu, Y., Tang, Q., et al. (2021). Impacts of meteorology and emission variations on the heavy air pollution episode in North China around the 2020 Spring Festival. *Science China Earth Sciences*, 64(2), 329–339. <https://doi.org/10.1007/s11430-020-9683-8>

Yan, Q., Wang, Y., Cheng, Y., & Li, J. (2021). Summertime clean-background ozone concentrations derived from ozone precursor relationships are lower than previous estimates in the Southeast United States. *Environmental Science & Technology*, 55(19), 12852–12861. <https://doi.org/10.1021/acs.est.1c03035>

Yang, X., Wang, Q., Liu, L., Tian, J., Xie, H., Wang, L., et al. (2025). Impacts of emission reduction and meteorological conditions on air quality improvement from 2016 to 2020 in the Northeast Plain, China. *Journal of Environmental Sciences*, 151, 484–496. <https://doi.org/10.1016/j.jes.2024.04.017>

Yao, L., Wang, D., Fu, Q., Qiao, L., Wang, H., Li, L., et al. (2019). The effects of firework regulation on air quality and public health during the Chinese Spring Festival from 2013 to 2017 in a Chinese megacity. *Environment International*, 126, 96–106. <https://doi.org/10.1016/j.envint.2019.01.037>

Zhang, F., Xu, X., Quan, W., Hu, Y., Zhang, B., Yuan, F., & Zhou, J. (2024). Comparison of two extreme rainfall/snowfall and freezing weather events during the Spring Festival transportation period in 2024. *Torrential Rain and Disasters*, 43(4), 371–383. <https://doi.org/10.12406/byzh.2024.095>

Zhang, J., & Wu, L. (2018). The influence of population movements on the urban relative humidity of Beijing during the Chinese Spring Festival holiday. *Journal of Cleaner Production*, 170, 1508–1513. <https://doi.org/10.1016/j.jclepro.2017.09.274>

Zhao, F. (2025). CNEMC O_3 NO_2 . figshare, Collection. <https://doi.org/10.6084/m9.figshare.29886155.v1>

Zheng, B., Cheng, J., Geng, G., Wang, X., Li, M., Shi, Q., et al. (2021). Mapping anthropogenic emissions in China at 1 km spatial resolution and its application in air quality modeling. *Science Bulletin*, 66(6), 612–620. <https://doi.org/10.1016/j.scib.2020.12.008>

References From the Supporting Information

Gu, C., Zhang, L., Xu, Z., Xia, S., Wang, Y., Li, L., et al. (2023). High-resolution regional emission inventory contributes to the evaluation of policy effectiveness: A case study in Jiangsu Province, China. *Atmospheric Chemistry and Physics*, 23(7), 4247–4269. <https://doi.org/10.5194/acp-23-4247-2023>

Xu, R., Ma, H., Li, J., Tong, D., Yan, L., Wang, L., et al. (2025). A technology-based global non-methane volatile organic compounds (NMVOC) emission inventory under the MEIC framework. *EGUphere*, 2025, 1–30. <https://doi.org/10.5194/egusphere-2025-1085>